ADVANCED MATERIALS
www.advmat.de

Room-Temperature-Formed PEDOT:PSS Hydrogels Enable Injectable, Soft, and Healable Organic Bioelectronics

Shiming Zhang, Yihang Chen, Hao Liu, Zitong Wang, Haonan Ling, Changsheng Wang, Jiahua Ni, Betül Çelebi-Saltik, Xiaochen Wang, Xiang Meng, Han-Jun Kim, Avijit Baidya, Samad Ahadian, Nureddin Ashammakhi, Mehmet R. Dokmeci, Jadranka Travas-Sejdic, and Ali Khademhosseini**

There is an increasing need to develop conducting hydrogels for bioelectronic applications. In particular, poly(3,4-ethylenedioxythiophene): poly(styrenesulfonate) (PEDOT:PSS) hydrogels have become a research hotspot due to their excellent biocompatibility and stability. However, injectable PEDOT:PSS hydrogels have been rarely reported. Such syringe-injectable hydrogels are highly desirable for minimally invasive biomedical therapeutics. Here, an approach is demonstrated to develop injectable PEDOT:PSS hydrogels by taking advantage of the room-temperature gelation property of PEDOT:PSS. These PEDOT:PSS hydrogels form spontaneously after syringe injection of the PEDOT:PSS suspension into the desired location, without the need of any additional treatments. A facile strategy is also presented for large-scale production of injectable PEDOT:PSS hydrogel fibers at room temperature. Finally, it is demonstrated that these room-temperature-formed PEDOT:PSS hydrogels (RT-PEDOT:PSS hydrogel) and hydrogel fibers can be used for the development of soft and self-healable hydrogel bioelectronic devices.

Conducting polymer poly(3,4-ethylenedioxythiophene) doped with poly(styrene sulfonate) (PEDOT:PSS) has gained great success in the past years due to its biocompatibility, high conductivity, and water stability.[1] Advances in research on PEDOT:PSS have unveiled its extensive applications for various functional devices, such as solar cells,[2] light-emitting diodes,[3] transparent electrodes,[4] electrochemical transistors,[5] memristors,[6] and supercapacitors.[7] Recently, we have witnessed an emerging trend of flexible electronics where PEDOT:PSS plays a key role in developing soft bioelectronic devices that can directly interface with the human body thanks to its inherently superior flexibility compared to its inorganic counterparts.[8] Despite these successes, the majority of bioelectronic devices still

Dr. S. Zhang, H. Liu, Z. Wang, Dr. J. Ni, Prof. B. Çelebi-Saltik, X. Wang, Dr. H.-J. Kim, Dr. A. Baidya, Dr. S. Ahadian, Prof. A. Khademhosseini
Department of Bioengineering
University of California-Los Angeles
Los Angeles, CA 90095, USA
E-mail: zhangshimingjlu@gmail.com; khademh@ucla.edu

Dr. S. Zhang, Y. Chen, H. Liu, Z. Wang, H. Ling, Dr. J. Ni, Prof. B. Çelebi-Saltik, X. Wang, Dr. H.-J. Kim, Dr. A. Baidya, Dr. S. Ahadian, Prof. N. Ashammakhi, Prof. M. R. Dokmeci, Prof. A. Khademhosseini
Center for Minimally Invasive Therapeutics (C-MIT)
University of California-Los Angeles
Los Angeles, CA 90095, USA

Dr. S. Zhang, Y. Chen, H. Liu, Z. Wang, H. Ling, Dr. J. Ni, Prof. B. Çelebi-Saltik, X. Wang, Dr. H.-J. Kim, Dr. A. Baidya, Dr. S. Ahadian, Prof. N. Ashammakhi, Prof. M. R. Dokmeci, Prof. A. Khademhosseini
California NanoSystems Institute
University of California-Los Angeles
Los Angeles, CA 90095, USA

Y. Chen
Department of Materials Science and Engineering
University of California-Los Angeles
Los Angeles, CA 90095, USA

The ORCID identification number(s) for the author(s) of this article can be found under https://doi.org/10.1002/adma.201904752.

DOI: 10.1002/adma.201904752

H. Liu
The Key Laboratory of Biomedical Information Engineering of Ministry of Education
School of Life Science and Technology
Xi'an Jiaotong University
Xi'an 710049, P. R. China

H. Liu
Bioinspired Engineering and Biomechanics Center (BEBC)
Xi'an Jiaotong University
Xi'an 710049, P. R. China

H. Ling
Department of Mechanical and Aerospace Engineering
University of California-Los Angeles
Los Angeles, CA 90095, USA

Dr. C. Wang
Department of Chemistry
University of Montreal
Montreal, QC H3T 2B1, Canada

Prof. B. Çelebi-Saltik
Department of Stem Cell Sciences, Graduate School of Health Sciences
Hacettepe University
Sihhiye, 06100 Ankara, Turkey

Dr. X. Meng
Department of Engineering Physics
Polytechnique Montreal
Montreal, QC H3C 3A7, Canada

rely on PEDOT:PSS in the form of thin films, which are physically and mechanically dissimilar to biological tissues. Such physical and mechanical mismatches may pose potential difficulties in forming natural integration with biological tissues via long-term stable and conformal interfaces.[9] Thus, establishing a PEDOT:PSS-based bioelectronic interface with improved tissue-like properties will greatly promote its application in the field of soft bioelectronics.

Compared to thin films, PEDOT:PSS hydrogels are considered as more ideal interfacing alternatives to biological tissues because of their water-rich nature and tissue-like mechanical properties. They not only provide a suitable microenvironment for cell growth and differentiation, but also have an electrically conductive network that allows for the in situ investigation of cellular behaviors under electrical stimulation.[10] Correspondingly, tremendous attention has been paid to investigate the fundamental properties of PEDOT:PSS hydrogels. In this content, Shi and co-workers synthesized conductive PEDOT:PSS hydrogels by mixing a PEDOT:PSS suspension with concentrated H_2SO_4 at an elevated temperature of 90 °C.[11] High performance supercapacitors were constructed by using these hydrogels as electrodes. Bao and co-workers demonstrated a method to make interpenetrating networks in PEDOT:PSS hydrogels to tune their mechanical properties for better integration with biological tissues.[9b] Zhao and co-workers reported pure PEDOT:PSS hydrogels by controlled dry-annealing and rehydration of PEDOT:PSS thin films. High swelling ratio was obtained in the thickness direction without mechanical constraints.[9a] In addition, Xu and co-workers proposed a multifunctional hydrogel based on PEDOT:PSS, which showed excellent photothermal conversion and stretchability via one-step polymerization.[12] Finally, Zhao and co-workers reported highly stretchable PEDOT:PSS hydrogel microfibers fabricated with multiflow microfluidics.[13] Despite these results, most of these hydrogels were fabricated at elevated temperatures which were beyond the tolerance limit of biological tissues. PEDOT:PSS hydrogels that can be formed spontaneously at room temperature (RT-PEDOT:PSS hydrogels) are highly favorable for direct processing and patterning under temperature-sensitive environments.[9b,14] We hypothesize that a proper manipulation of an RT-PEDOT:PSS hydrogel could enable the development of injectable hydrogels where crosslinking and autonomous gelation can be controlled occurring only after the injection of PEDOT:PSS suspension into the desired location such as human body. Such injectable PEDOT:PSS hydrogels will be of great medical demand, especially for nerve regeneration and brain stimulation or recording. Further investigation on the fundamental properties of these hydrogels may promote their applications in next-generation organic and hydrogel bioelectronics.

In this communication, we present a strategy to develop injectable conductive hydrogels by taking advantage of the room-temperature gelation ability of PEDOT:PSS suspension. Gelation of the PEDOT:PSS can be achieved spontaneously, at room temperature, after syringe-injecting surfactant-mixed PEDOT:PSS suspension into the desired location, without any additional treatments. A facile method for large-scale production of injectable PEDOT:PSS hydrogel fibers is presented by injecting and crosslinking the PEDOT:PSS suspension within a confined cylinder tube. We demonstrate that these hydrogel fibers can be used as electroactive materials to develop organic bioelectronic devices such as organic electrochemical transistors (OECTs). Moreover, we reveal that these RT-PEDOT:PSS hydrogels own high volumetric swelling ratios, which can be further used for water-healable hydrogel bioelectronics.

RT-PEDOT:PSS hydrogels were obtained by simply mixing PEDOT:PSS suspension with 4-dodecylbenzenesulfonic acid (DBSA), which is a widely used secondary dopant (surfactant) in processing PEDOT:PSS. Spontaneous gelation occurred when the concentration of DBSA reached a threshold value of ≈3 v/v%, without further treatment (**Figure 1**a,b). The time required for the gelation was controllable between 2 and 200 min, depending on the concentration of DBSA (Figure S1, Supporting Information). The formation of PEDOT:PSS hydrogels at room temperature is tentatively attributed to the physical crosslinking between $PEDOT^+$ polymer chains,[11,14] enabled by the addition of DBSA (Figure 1c). It is known that PEDOT:PSS has a core–shell structure. The coiled and hydrophilic PSS^- shell surrounds the hydrophobic $PEDOT^+$, and the complex forms a suspension in water.[15] $PEDOT^+$ and PSS^- chains interact via electrostatic interactions.[14] DBSA is an acidic surfactant which, once the concentration value is more than the critical micelle concentration (Figure 1c),[16] is capable of forming well-defined micellar structures in water, headed with negatively charged sulfuric acid groups (SO_3^-). The presence of sufficient DBSA molecules, as indicated by Fourier-transform infrared spectroscopy (FTIR) (Figure S2, Supporting Information), increases the ionic strength in the solution and provides sufficient H^+ to protonate the PSS^-. The increased ionic strength is supposed to weaken the electrostatic attraction between $PEDOT^+$ and PSS^- chains,[14] which subsequently exposes $PEDOT^+$ chains to each other and promotes their interchain interactions to form a connected 3D network (Figure 1c) due to physical crosslinking induced by π–π stacking and hydrophobic attractions. Complex viscosity in physically crosslinked hydrogels normally decreases upon increasing shear frequency. This was confirmed by the result where we observed a decrease in complex viscosity of more than two orders of magnitude when increasing the shear frequency from 0.1 to 10 rad s^{-1} (Figure S3, Supporting Information). Despite a relatively weak physical crosslinking in these hydrogels, they could be manipulated into 3D, self-standing structures with various shapes (Figure S4, Videos S1 and S2, Supporting Information).

Prof. N. Ashammakhi, Prof. M. R. Dokmeci, Prof. A. Khademhosseini
Department of Radiology
University of California-Los Angeles
Los Angeles, CA 90095, USA
Prof. J. Travas-Sejdic
Polymer Electronic Research Centre
School of Chemical Sciences
The University of Auckland
23 Symonds Street, Auckland 1023, New Zealand
Prof. J. Travas-Sejdic
MacDiarmid Institute for Advanced Materials and Nanotechnology
Kelburn Parade
Wellington 6140, New Zealand
Prof. A. Khademhosseini
Department of Chemical and Biomolecular Engineering
University of California-Los Angeles
Los Angeles, CA 90095, USA

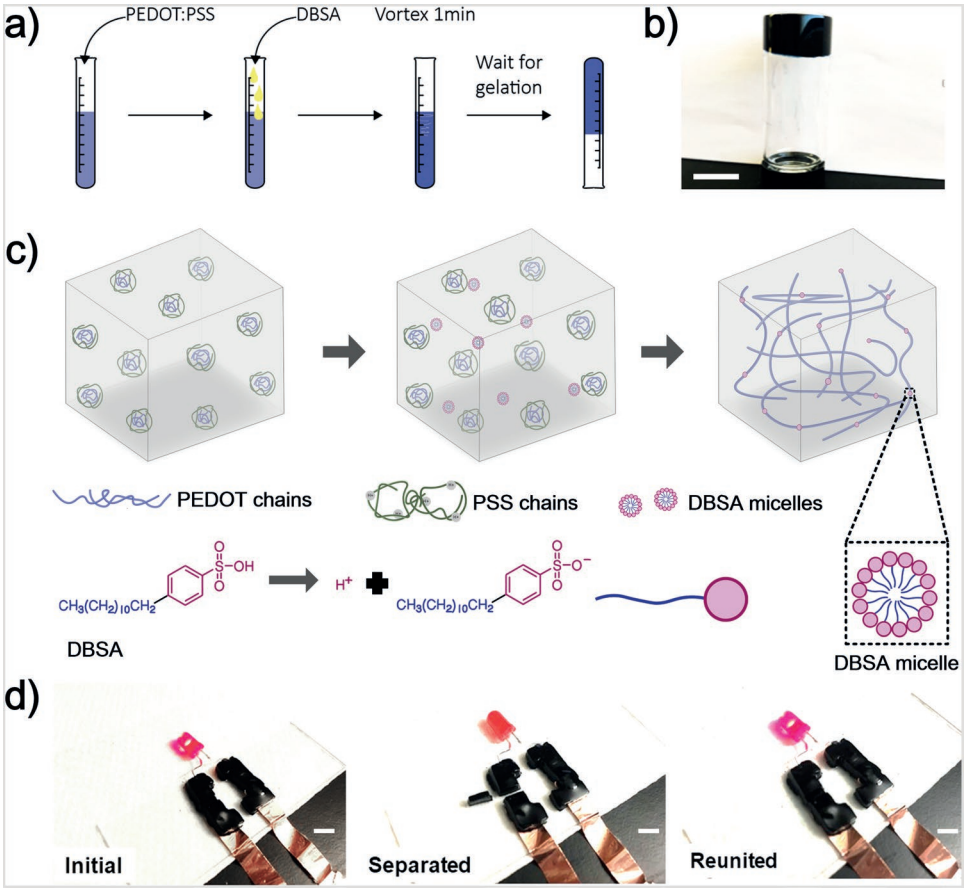

Figure 1. a) Schematic illustration of gelation processes of RT-PEDOT:PSS hydrogel. b) RT-PEDOT:PSS hydrogel formed after 10 min (4 v/v% DBSA): the gel adhered at the bottom when flipping the vial. c) Crosslinking mechanism of our RT-PEDOT:PSS hydrogel. The addition of the DBSA into the suspension weakens electrostatic attraction between $PEDOT^+$ and PSS^-, exposing the $PEDOT^+$ chains to water. The exposed $PEDOT^+$ chains undergo a conformational change from a confined-coiled to an expanded-linear structure and subsequently physically crosslinked due to π–π stacking and hydrophobic attractions. d) RT-PEDOT:PSS hydrogels acting as conductive interconnects to drive a LED via a "cut and stick" approach. Scale bar: 5 mm.

The RT-PEDOT:PSS hydrogel showed a moderate conductivity of $\approx 10^{-1}$ S cm^{-1} (Figure S5, Supporting Information). Although it is lower than a PEDOT:PSS thin film (>1 S cm^{-1}),[17] it has already surpassed those values of most tissues in the brain or spinal cord where these hydrogels are expected to functionalize.[18] For example, the cerebrospinal fluid (CSF) holds the highest conductivity among human tissues. However, its value (15.38×10^{-3} S cm^{-1}) is still much lower than the RT-PEDOT:PSS hydrogels,[18] suggesting the conductivity should not be a limiting factor for future in vivo applications. Moreover, in practical applications, these hydrogels are expected to be used in the form of a thick gel, which will further lower their resistance compared to thin films. For example, as shown in Figure 1d and Video S3 (Supporting Information), RT-PEDOT:PSS hydrogels with a thickness of 5 mm had a total resistance of less than 100 ohm (Figure S6, Supporting Information) and was able to serve as interconnects to switch on a light-emitting diode (LED). Interestingly, the brightness of the LED was insensitive to external cuts in the hydrogel interconnects (Video S3, Supporting Information), attributable to their favorable viscoelastic property. The current flowing across the RT-PEDOT:PSS hydrogel could only be interrupted by removing a bulky piece of the hydrogel from the circuit (Figure 1d; Video S3, Supporting Information). Importantly, the current was able to recover to its initial value when we pushed the hydrogel piece back to the circuit, demonstrating these RT-PEDOT:PSS hydrogels could be manipulated in a customized "cut and stick" approach.

The unique room-temperature gelation ability of PEDOT:PSS enables us to demonstrate injectable PEDOT:PSS hydrogels,[19] which can find potential applications in minimally invasive therapeutics such as nerve regeneration and brain stimulation, without causing any trauma.[20] As a demonstration, we first injected the PEDOT:PSS suspension (premixed with DBSA) into a void polydimethylsiloxane (PDMS) mold with a syringe (**Figure 2**a and Video S4, Supporting Information). RT-PEDOT:PSS hydrogels formed spontaneously in the mold after completing the injection process. These PEDOT:PSS hydrogels stayed stably in the mold even after inversion (Figure 2a). The RT-PEDOT:PSS hydrogel also enables the direct fabrication of conductive interconnects on temperature-sensitive substrates such as gelatin, a skin-derived hydrogel that cannot tolerate heating because of its low melting temperature around 37 °C. To make conductive interconnects in gelatin with

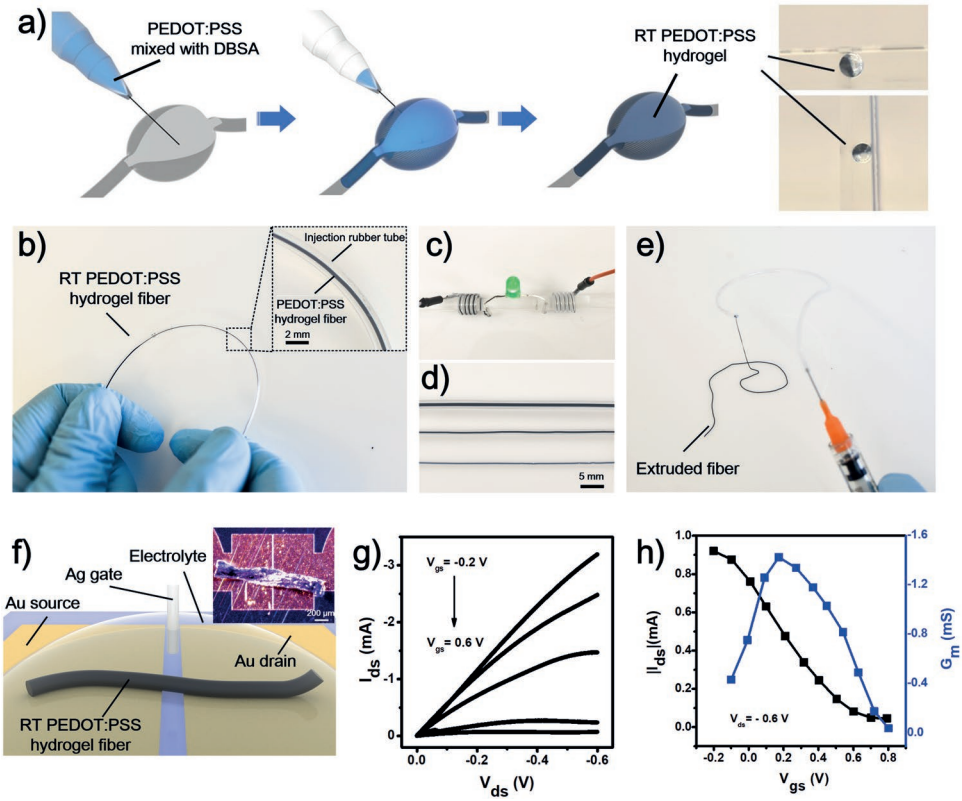

Figure 2. a) Schematic of injectable RT-PEDOT:PSS hydrogels: Puncturing the soft tissue with syringe; Syringe-injecting PEDOT:PSS suspension (4 v/v% DBSA) into the cavity; and RT-PEDOT:PSS hydrogel formed spontaneously within 10 min. The optical images show the RT-PEDOT:PSS hydrogel attached to the wall of the cavity even when we tilted the mold. b) Formation of the RT-PEDOT:PSS hydrogel in a plastic tube via syringe injection. Inset: enlarged view of the RT-PEDOT:PSS hydrogel in tube. c) Application of RT-PEDOT:PSS hydrogel fibers for driving an LED. d) Injectable RT-PEDOT:PSS hydrogel fibers with different diameters of 875, 480, and 400 μm. e) Extruded RT-PEDOT:PSS hydrogel fibers with a syringe. f) Schematic of the fabricated OECTs with injected RT-PEDOT:PSS hydrogel fiber. The hydrogel fiber was freeze-dried after printing on the Au electrodes which have a gap of 10 μm; the inset shows the real optical image of the freeze-dried fiber on the source–drain electrodes. g,h) Output and transfer curves of the OECTs with RT-PEDOT:PSS hydrogel fibers as the channel.

the injectable PEDOT:PSS hydrogel, serpentine channels were first created in the gelatin (Figure S7, Supporting Information). Next, the PEDOT:PSS suspension was injected into these channels and hydrogel interconnects were subsequently obtained. These serpentine RT-PEDOT:PSS hydrogels in gelatin could tolerate mechanical deformations such as bending and twisting without breaking. The current flow through the RT-PEDOT:PSS hydrogel maintained 80% of its initial value even after being strained up to 50% (Figure S7, Supporting Information).

The Young's modulus of the obtained RT-PEDOT:PSS hydrogel is ≈1 kPa (Figure S8a,d, Supporting Information), whereas the modulus of biological tissues in human body ranges from 1 to 100 kPa.[21] Therefore, an improved mechanical property could potentially minimize the mechanical mismatch between injectable hydrogel and various human tissues. We increased mechanical strength of the injectable RT-PEDOT:PSS hydrogel by infiltrating it with precursors of a secondary hydrogel (polyacrylamide, PAAm) (Figure S9, Supporting Information).[9b,22] The robust, covalent-bonded network in the PAAm hydrogel increased the modulus of the whole hydrogel by forming interpenetrating networks with the PEDOT:PSS hydrogel. Precursor of PAAm hydrogel was also manipulated to be injectable and crosslinkable at room temperature by using a unique initiator, the ammonium persulfate (APS) which could trigger the gelation of PAAm at 25 °C (Figure S9, Supporting Information).[23] With this method, we were able to control the Young's modulus of the RT-PEDOT:PSS hydrogel between 1 and 100 kPa (Figure S8d, Supporting Information), which covered the modulus range of most relevant tissues. For example, the brain has a Young's modulus of 1–4 kPa and the heart has a Young's modulus of 10–18 kPa.[21] Significantly, a comparable resistance was observed in the infiltrated hydrogel (Figure S6, Supporting Information), suggesting the secondary network had a minor effect in the conductivity due to preformed conductive paths in the PEDOT networks before infiltrating. These results outline the feasibility to develop mechanically robust and injectable PEDOT:PSS hydrogels at room temperature, endowing PEDOT:PSS with fresh features for potential biomedical applications.

To further demonstrate the diverse applications of these injectable RT-PEDOT:PSS hydrogels, we present a method to produce injectable hydrogel fibers by syringe-injecting and crosslinking PEDOT:PSS suspension into a plastic hollow tube (Figure 2b). The formed RT-PEDOT:PSS hydrogel fibers could be extruded by pressurizing the tube with controlled speed while maintaining their structural integrity because of

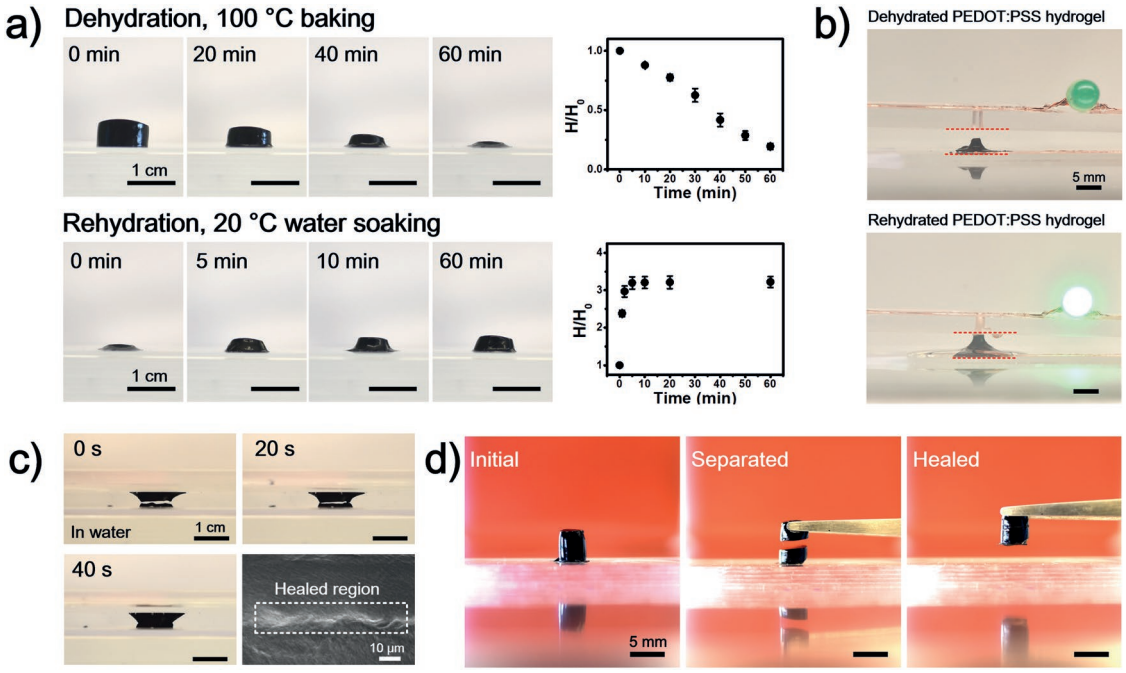

Figure 3. a) Volumetric shrinking and swelling properties of the RT-PEDOT:PSS hydrogels under mild dehydration (N = 3). b) Application of the swellable RT-PEDOT:PSS hydrogel as a water-controllable switch for an LED. c) Optical images of the healing processes of a damaged RT-PEDOT:PSS hydrogel, and SEM images of the healed region. d) Mechanical healing of the RT-PEDOT:PSS hydrogel by placing two separated RT-PEDOT:PSS hydrogels (mildly dehydrated) together for 5 min.

their good mechanical properties and the lubricating effect of the DBSA. Hydrogel fibers of adjustable diameters could be obtained by using plastic tubes with different sizes (Figure 2c–e). These hydrogel fibers could be manipulated into various shapes through the syringe by simply hand-writing (Figure S10, Supporting Information). It is worth mentioning that these hydrogel fibers could be injected into an aqueous solution in a way similar to wet spinning while maintaining their shapes even after entangling together (Videos S5 and S6, Supporting Information).

As a potential application, we exploited the possibility of using RT-PEDOT:PSS hydrogel fibers as channel material for the fabrication of organic bioelectronic device, such as OECT, which has been widely used for in vivo bioelectronics studies.[5] The OECT was fabricated by simply syringe-injecting an RT-PEDOT:PSS hydrogel fiber between two metallic electrodes, followed by a freeze-drying process (Figure 2f). The output and transfer curves of the OECT are shown in Figure 2g,h. The OECT showed typical transistor behavior working in the depletion mode. The resultant OECT had a maximum transconductance of ≈1.4 mS (V_{ds} = −0.6 V, V_{gs} = −0.2 V) (Figure 2h), which was comparable to conventional OECTs based on PEDOT:PSS thin films.[24] These results demonstrate good electrochemical properties of these PEDOT:PSS hydrogel fibers, indicating their potential applications for organic and hydrogel bioelectronics.

Recently we have discovered that PEDOT:PSS in the form of thin films demonstrated self-healing properties due to its excellent volumetric swelling ability upon exposing to water.[25] Accordingly, we investigated the volumetric swelling property in these RT-PEDOT:PSS hydrogels. Strikingly, we observed that these hydrogels showed greater volumetric swelling abilities compared to thin films. As shown in **Figure 3**a, the height of a dehydrated RT-PEDOT:PSS hydrogel (100 °C, 1 h), swelled remarkably to ≈300% of its initial value within ≈5 min. Hydrogels dehydrated at room-temperature also showed high volumetric swelling ratio, regardless of their initial shapes (Figure S11, Supporting Information). As a demonstration for self-healing hydrogel electronics, we placed a dehydrated PEDOT:PSS hydrogel between two conductive copper tapes that adhered to glass slides (Figure 3b). No current flow was observed in the circuit due to the gap between the hydrogel and the top electrode. Subsequently, we hydrated the device with water, which induced swelling of the PEDOT:PSS hydrogel and led to its physical connection to the top electrode, thereby switching on the LED. The healing process was further demonstrated by cutting the RT-PEDOT:PSS hydrogel with a razor blade, which created a gap of about 1 mm (Figure 3c). The presence of water healed the gap within only 40 s due to the rapid swelling of the RT-PEDOT:PSS hydrogel (Video S7, Supporting Information). Additionally, the mechanical healing of RT-PEDOT:PSS hydrogels was achieved by connecting two separated hydrogels together. After 5 min, these two separated PEDOT:PSS hydrogels healed together and could be lifted up with tweezers (Figure 3d). Overall, these results demonstrate that these RT-PEDOT:PSS hydrogels are promising candidates for self-healing electronics.

Finally, we evaluated biocompatibility of RT-PEDOT:PSS hydrogels by culturing C2C12 muscle cells on their surface to assess the cytotoxicity. Before the cell culture, the gel-coated poly(ethylene terephthalate) (PET) substrate was rinsed thoroughly in Dulbecco's phosphate-buffered saline (DPBS) media to remove any access acidic residue. Cell viability and proliferation analyses were carried out at a density of 100 000 cells per well.

The cells proliferated on the RT-PEDOT:PSS hydrogel surfaces after 3 d, and only a slight difference was observed between cells cultured on reference surfaces and cells cultured on these hydrogel surfaces (Figure S5, Supporting Information). These results indicate that RT-PEDOT:PSS hydrogels may provide a suitable environment for cell growth, thus ensuring their use towards biological applications.[26]

We have presented a strategy to obtain injectable PEDOT:PSS hydrogels by using room-temperature crosslinkable PEDOT:PSS suspension. We have demonstrated that these injectable PEDOT:PSS hydrogels can be potentially used to obtain injectable conductors into human tissue, stretchable interconnects on temperature-sensitive substrates, and water-healable hydrogel conductors by taking advantage of their high volumetric swelling ratios. We also demonstrated that these injectable hydrogels could enable the development of PEDOT:PSS hydrogel fibers, which could be used to develop future hydrogel bioelectronic devices such as hydrogel-based OECTs. Further investigations and optimizations on the electrical and mechanical properties of these injectable PEDOT:PSS hydrogels and hydrogel fibers will promote their uses toward biomedical applications.

Experimental Section

Materials: PEDOT:PSS (Clevios PH1000) was purchased from Haraeus Electronic Materials, Germany. DBSA, gelatin from porcine skin, and gallium–indium eutectic (EGaIn) were purchased from Sigma Aldrich, USA. DPBS was purchased from Gibco, USA.

Synthesis of RT-PEDOT:PSS Hydrogels: The PEDOT:PSS hydrogels were obtained by adding 4 v/v% of DBSA solution into the PEDOT:PSS (suspension), followed by agitation. Then, the mixture was poured into prepatterned molds and then placed in a desiccator or centrifuged to remove bubbles induced by vortex. PEDOT:PSS hydrogels formed spontaneously within about 10 min after mixing DBSA (4 v/v%) with PEDOT:PSS suspension. Gelation time was defined by tube inversion method.

Characterization of RT-PEDOT:PSS Hydrogel: The tensile test of the RT-PEDOT:PSS hydrogel was implemented with the INSTRON tensile tester (INSTRON 5943, USA) in extension mode (extension rate of 1 mm min^{-1}).

Rheology tests were performed with the Anton-Paar rheometer (MCR 302, Austria). All samples had a diameter of 8 mm and height of 3 mm. The samples were cut by a circular blade and had a diameter of 8 mm. The storage and loss modulus as well as complex viscosity were measured via small amplitude shear oscillation with constant shear rates (0.1–10 rad s^{-1}) in the linear region. The infiltration process for increasing the mechanical property of the RT-PEDOT:PSS hydrogel is detailed in Figure S9 (Supporting Information).

The conductivity of RT-PEDOT:PSS hydrogel was characterized by biasing the hydrogel at a constant direct current (DC) voltage of 1 V with the source measure unit Agilent B2901A (Keysight Technologies, USA). Conductive copper tape and EGaIn were used to connect the PEDOT:PSS hydrogel (length × width × thickness: 20 mm × 20 mm × 5 mm) to the source measure unit. The current was collected after biasing the PEDOT:PSS hydrogel for 100 s at 1 V, which allowed us to extract a stable DC conductance. Conductivity of the dehydrated PEDOT:PSS hydrogel was measured after oven-baking the gel at 100 °C for 1 h. The length, width, and thickness of RT-PEDOT:PSS hydrogels for conductivity characterization are 20, 20,and 5 mm, respectively.

The electromechanical properties of patterned PEDOT:PSS hydrogels on gelatin substrates were tested with a tensile tester. Liquid metal (EGaIn) and conductive tape (3M 9703) were used to facilitate the electrical connection to the samples.

Biocompatibility Evaluation of RT-PEDOT:PSS Hydrogel: Cell culture was performed with C2C12 cells (mouse muscle cells). Cells were seeded on RT-PEDOT:PSS hydrogel coated and uncoated PET surfaces as control. A live/dead calcein AM/ethidium homodimer assay (Thermo Scientific) was used to quantify the viability of the cells according to the manufacturer instruction until day-3. Cell proliferation was quantified using Presto Blue (Thermo Scientific) by measuring the metabolic activity of cells until day 7. 100 µL of staining solution for each condition was transferred into ELISA (enzyme-linked immunosorbent assay) microplates (96-well plates, Corning Life Sciences, Lowell, MA, USA) for spectrophotometric measurement. The absorbance of the solutions was measured spectrophotometrically at 570 nm.

Patterning of RT-PEDOT:PSS Hydrogel: Patterned RT-PEDOT:PSS hydrogels were obtained with laser ablated PMMA molds (VLS 2.30, Universal Laser, USA). For pattering on gelatin, patterned and stretchable gelatin substrate was first obtained with a PMMA mold. Next, PEDOT:PSS solution (with 4 v/v% DBSA) was quickly syringe-injected into the microchannels in gelatin substrate. PEDOT:PSS hydrogels formed spontaneously in gelatin microchannels within 10 min after injection.

Fabrication of OECTs with RT-PEDOT:PSS Hydrogel Fibers: Silicon substrates were precleaned with acetone, IPA, and DI water. Then photoresist (SPR 700 1.2) was spin-coated on top of the substrates, followed by UV exposure under an optical shadow mask to define the desired patterns. After photoresist developing (MA-26A, 30s), Ti/Au (10 nm/100 nm) was deposited. Patterned source and drain electrodes were obtained after stripping the photoresist with acetone in a sonication bath. Next, parylene was selectively deposited on top of the electrodes as insulating layer. The RT-PEDOT:PSS hydrogel fiber was subsequently syringe-injected between the source and drain electrode as the transistor channel, followed by a freeze-drying process. The channel length is 10 µm, the channel width is 1000 µm, and the diameter of the RT-PEDOT:PSS hydrogel is about 200 µm, which shrinks to 20 µm after baking (100 °C, 1 h). Before transistor measurements, chitosan solution was coated on top of the freeze-dried RT-PEDOT:PSS hydrogel to prevent delamination during the experiments. Finally, a silver wire was inserted into cetyltrimethylammonium bromide (CTAB) solution as gate electrode. The characterization of the OECTs was performed with Agilent B2902A, controlled with LabVIEW software for output and transfer curves measurements.

Supporting Information

Supporting Information is available from the Wiley Online Library or from the author.

Acknowledgements

S.Z., Y.C., and H.L. contributed equally to this work. This work is supported by the National Institutes of Health (Grant Nos. 1R01HL140951-01A1 and 1R01HL140618-01). The authors would like to thank Prof. Halima Alem for discussions on the gelation of the hydrogel.

Note: The presentation of the author name Betül Çelebi-Saltik was corrected and the eighth affiliation added on January 7, 2020, after initial publication online. In addition the text was updated to refer to the PEDOT:PSS suspension, rather than PEDOT:PSS liquid throughout. Furthermore, the text was updated on pages 2 to 7 to correct the tense in some places and correct some typos. Specifically, memristors are cited to ref. [6] on page 1.

Conflict of Interest

The authors declare no conflict of interest.

Keywords

healable, injectable, minimally invasive, PEDOT:PSS hydrogel

Received: July 24, 2019
Revised: September 23, 2019
Published online: October 28, 2019

[1] L. Groenendaal, F. Jonas, D. Freitag, H. Pielartzik, J. R. Reynolds, *Adv. Mater.* **2000**, *12*, 481.
[2] a) Y. H. Kim, C. Sachse, M. L. Machala, C. May, L. Müller-Meskamp, K. Leo, *Adv. Funct. Mater.* **2011**, *21*, 1076; b) D. J. Lipomi, B. C.-K. Tee, M. Vosgueritchian, Z. Bao, *Adv. Mater.* **2011**, *23*, 1771.
[3] Y.-S. Liu, J. Feng, X.-L. Ou, H.-f. Cui, M. Xu, H.-B. Sun, *Org. Electron.* **2016**, *31*, 247.
[4] X. Crispin, F. L. E. Jakobsson, A. Crispin, P. C. M. Grim, P. Andersson, A. Volodin, C. van Haesendonck, M. Van der Auweraer, W. R. Salaneck, M. Berggren, *Chem. Mater.* **2006**, *18*, 4354.
[5] J. Rivnay, S. Inal, A. Salleo, R. M. Owens, M. Berggren, G. G. Malliaras, *Nat. Rev. Mater.* **2018**, *3*, 17086.
[6] a) Y. van de Burgt, E. Lubberman, E. J. Fuller, S. T. Keene, G. C. Faria, S. Agarwal, M. J. Marinella, A. Alec Talin, A. Salleo, *Nat. Mater.* **2017**, *16*, 414; b) E. J. Fuller, S. T. Keene, A. Melianas, Z. Wang, S. Agarwal, Y. Li, Y. Tuchman, C. D. James, M. J. Marinella, J. J. Yang, A. Salleo, A. A. Talin, *Science* **2019**, *364*, 570.
[7] G. S. Gund, J. H. Park, R. Harpalsinh, M. Kota, J. H. Shin, T.-I. Kim, Y. Gogotsi, H. S. Park, *Joule* **2019**, *3*, 164.
[8] L. V. Kayser, D. J. Lipomi, *Adv. Mater.* **2019**, *31*, 1806133.
[9] a) B. Lu, H. Yuk, S. Lin, N. Jian, K. Qu, J. Xu, X. Zhao, *Nat. Commun.* **2019**, *10*, 1043; b) V. R. Feig, H. Tran, M. Lee, Z. Bao, *Nat. Commun.* **2018**, *9*, 2740.
[10] a) A. R. Spencer, A. Primbetova, A. N. Koppes, R. A. Koppes, H. Fenniri, N. Annabi, *ACS Biomater. Sci. Eng.* **2018**, *4*, 1558; b) C. Tondera, T. F. Akbar, A. K. Thomas, W. Lin, C. Werner, V. Busskamp, Y. Zhang, I. R. Minev, *Small* **2019**, *15*, 1901406.
[11] B. Yao, H. Wang, Q. Zhou, M. Wu, M. Zhang, C. Li, G. Shi, *Adv. Mater.* **2017**, *29*, 1700974.
[12] S. Cao, X. Tong, K. Dai, Q. Xu, *J. Mater. Chem. A* **2019**, *7*, 8204.
[13] J. Guo, Y. Yu, H. Wang, H. Zhang, X. Zhang, Y. Zhao, *Small* **2019**, *15*, 1805162.
[14] M. A. Leaf, M. Muthukumar, *Macromolecules* **2016**, *49*, 4286.
[15] J. Zhou, D. H. Anjum, L. Chen, X. Xu, I. A. Ventura, L. Jiang, G. Lubineau, *J. Mater. Chem. C* **2014**, *2*, 9903.
[16] M. S. Khan, Z. Ali, *Chin. J. Polym. Sci.* **2005**, *23*, 29.
[17] S. Zhang, P. Kumar, A. S. Nouas, L. Fontaine, H. Tang, F. Cicoira, *APL Mater.* **2015**, *3*, 014911.
[18] C. Ramon, P. H. Schimpf, J. Haueisen, *BioMed. Eng. OnLine* **2006**, *5*, 10.
[19] J. Liu, T.-M. Fu, Z. Cheng, G. Hong, T. Zhou, L. Jin, M. Duvvuri, Z. Jiang, P. Kruskal, C. Xie, Z. Suo, Y. Fang, C. M. Lieber, *Nat. Nanotechnol.* **2015**, *10*, 629.
[20] a) N. Ashammakhi, S. Ahadian, M. A. Darabi, M. El Tahchi, J. Lee, K. Suthiwanich, A. Sheikhi, M. R. Dokmeci, R. Oklu, A. Khademhosseini, *Adv. Mater.* **2019**, *31*, 1804041; b) W. Sun, J. Lee, S. Zhang, C. Benyshek, M. R. Dokmeci, A. Khademhosseini, *Adv. Sci.* **2019**, *6*, 1801039.
[21] A. M. Handorf, Y. Zhou, M. A. Halanski, W.-J. Li, *Organogenesis* **2015**, *11*, 1.
[22] a) J. Goding, A. Gilmour, P. Martens, L. Poole-Warren, R. Green, *Adv. Healthcare Mater.* **2017**, *6*, 1601177; b) H. Yuk, B. Lu, X. Zhao, *Chem. Soc. Rev.* **2019**, *48*, 1642; c) H. Warren, *MRS Proc.* **2013**, *1569*, 219; d) J.-Y. Sun, X. Zhao, W. R. Illeperuma, O. Chaudhuri, K. H. Oh, D. J. Mooney, J. J. Vlassak, Z. Suo, *Nature* **2012**, *489*, 133.
[23] a) S. H. Huang, S. Sheth, E. Jain, X. Jiang, S. P. Zustiak, L. Yang, *Opt. Express* **2018**, *26*, 51; b) E. Zhang, R. Bai, X. P. Morelle, Z. Suo, *Soft Matter* **2018**, *14*, 3563.
[24] S. Zhang, E. Hubis, C. Girard, P. Kumar, J. DeFranco, F. Cicoira, *J. Mater. Chem. C* **2016**, *4*, 1382.
[25] S. Zhang, F. Cicoira, *Adv. Mater.* **2017**, *29*, 1703098.
[26] Y. S. Zhang, A. Khademhosseini, *Science* **2017**, *356*, eaaf3627.